AGU PUBLICATIONS

JGR

Journal of Geophysical Research: Atmospheres

RESEARCH ARTICLE

10.1002/2014JD022513

Process-based assessment of an ensemble of climate projections for West Africa

Rachel James[1], **Richard Washington**[1], **and Richard Jones**[2,3]

[1]Climate Research Lab, Centre for the Environment, University of Oxford, Oxford, UK, [2]Met Office Hadley Centre, Exeter, UK, [3]School of Geography and the Environment, University of Oxford, Oxford, UK

Key Points:
- Circulation changes associated with modeled precipitation change are identified
- Modeled processes are similar for future change and historical variability
- Contrasts to variability in reanalyses bring these models' futures into question

Supporting Information:
- Figures S1–S9

Correspondence to:
R. James,
rachel.james@ouce.ox.ac.uk

Citation:
James, R., R. Washington, and R. Jones (2015), Process-based assessment of an ensemble of climate projections for West Africa, *J. Geophys. Res. Atmos.*, *120*, 1221–1238, doi:10.1002/2014JD022513.

Received 29 AUG 2014
Accepted 11 JAN 2015
Accepted article online 14 JAN 2015
Published online 16 FEB 2015

Abstract Determining the level of confidence in regional climate model projections could be very useful for designing climate change adaptation, particularly for vulnerable regions. The majority of previous research to evaluate models has been based on the mean state, but for confidence in projections the plausibility of the mechanisms for change is just as, if not more, important. In this study we demonstrate a methodology for process-based assessment of projections, whereby circulation changes accompanying future responses are examined and then compared to atmospheric dynamics during historical years in models and reanalyses. We apply this methodology to an ensemble of five global and regional model experiments and focus on West Africa, where these models project a strong drying trend. The analysis reveals that this drying is associated with anomalous subsidence in the upper atmosphere, and large warming of the Saharan heat low region, with potential feedback effects via the African easterly jet and West African monsoon. This mode occurs during dry years in the historical period, and dominates in the future experiments. However, the same mode is not found in dry years in reanalysis data, which casts doubt on the reasons for strong drying in these models. The regional models show a very similar response to their driving global models, and are therefore no more trustworthy in this case. This result underlines the importance of assessing model credibility on a case-by-case basis and implies that process-based methodologies should be applied to other model projections before their outputs are used to inform decision making.

1. Introduction

Examining the risks associated with anthropogenic climate change is a priority, particularly for vulnerable regions. Climate models provide an opportunity to investigate how regional climates might evolve in future; however, their simulations are subject to important uncertainties [see, e.g., *Hawkins and Sutton*, 2009], and their projections often diverge substantially, particularly in the case of precipitation [e.g., *Druyan*, 2011]. There are now an abundance of available data sets for future climate, including output from global climate models (GCMs) and regional climate models (RCMs), multimodel ensembles, and perturbed physics ensembles (PPEs). Together these represent a vast assortment of potential futures. So how should decision makers know which climate change projections to consider and which to disregard?

It is not a priori clear which models are more trustworthy. Models from different modeling centers, and different members of a PPE, each have their strengths and weaknesses. Regional models might be expected to generate more credible simulations than GCMs, due to the difficulty of reproducing finer-scale features with the large grid spacing of the latter. However, RCMs have their own uncertainties, and the 50 km experiments which are most commonly run [e.g., *Giorgi et al.*, 2009; *Jones et al.*, 2011; *Hewitson et al.*, 2012] still do not have high enough resolution to reproduce the key processes involved in tropical convection [*Marsham et al.*, 2013]. The ability of RCMs therefore deserves as much scrutiny as that of GCMs. So how should the validity of model projections be assessed?

The majority of studies designed to evaluate both GCMs and RCMs have been based on comparison between modeled hindcasts and historical observations [*Lau et al.*, 2006; *Nikulin et al.*, 2012; *Gbobaniyi et al.*, 2013]. Identifying biases can be used to eliminate clearly implausible models [*McSweeney et al.*, 2014] and aides understanding of responses to anthropogenic forcing, but examining modeled climatologies is not sufficient to assess model projections. Direct investigation of the mechanisms for future precipitation change is also important, and existing efforts in this area have generated valuable hypothesis about the potential drivers of wet and dry responses [e.g., *Biasutti et al.*, 2008, 2009; *Monerie et al.*, 2012a, 2012b].

Further work is needed for a more in-depth understanding of specific modeled signals, and this could also lead to an assessment of plausibility through comparison with interannual variability. Previous research into the generalized response of tropical precipitation to anthropogenic forcing has progressed using anomalously warm (El Niño) years as an analogue for future global warming [e.g., *Allan and Soden*, 2008]. If a model is able to capture the thermodynamic response associated with warm El Niño–Southern Oscillation events, this may shed light on its ability to respond to future warming. Regional precipitation responses might also be assessed by comparing mechanisms for precipitation change in historically wet and dry years with the future response. If a model shows wetting or drying in future for the same reasons as in the past, and the same mechanisms are found in observations, this might increase confidence in the model's response. Conversely, if the modeled processes associated with drying or wetting are different from processes identified in observations, it would give cause for concern.

In this paper we present a methodological framework for such analysis and apply it to an example. We have chosen an ensemble of five global and five regional model experiments developed by the Met Office Hadley Centre (MOHC) [*Buontempo et al*., 2014]. This model ensemble provides a unique opportunity to investigate future change, due to the relative consistency between the GCMs (which vary only in small perturbations to the atmospheric and land surface parameters), and between the GCM and the RCM, given the similarity in the underlying physics within the Unified Model family. This offers a distinct advantage over CMIP5 (Coupled Model Intercomparison project phase 5) [*Taylor et al*., 2012], for example, where there are many differences in model physics within the ensemble. Examining the Buontempo et al. data set is also important, as it is being employed in impacts and adaptation studies [e.g., *Jones et al*., 2012].

The assessment of this ensemble will focus on West Africa in July-August-September (JAS), as it is here that these models show the highest magnitude change: a large drying from western Sahel to west equatorial Africa [*James et al*., 2013, 2014]. Circulation anomalies associated with drying in West Africa in historical and future simulations will be investigated and compared to reanalysis data, to assess the credibility of the projected dry signal in the GCMs and the RCMs.

The aim of the paper is not to infer the most likely response in the Sahel. Model projections diverge substantially for this region, including spatially coherent dry signals in several Geophysical Fluid Dynamics Laboratory (GFDL) models and an equally large-scale wetting in the Model for Interdisciplinary Research on Climate (MIROC) [*Held et al*., 2005; *Cook and Vizy*, 2006]. Our goal is only to interrogate the specific projections from the MOHC ensemble, which might provide information about whether this particular dry signal represents a genuine risk to West Africa. If the methodology proves useful, it could also be applied to other models to build up an evidence base about plausible and implausible futures.

The MOHC ensemble will be described in the next section, followed by an analysis of the future precipitation projections from both the GCMs and the RCMs and an examination of the accompanying circulation changes, as a first step toward understanding why dryer futures are projected in these models. Section 4 will then present composites of historical dry (minus wet) years to determine whether the models show similar circulation changes associated with drying in the past as drying in the future, and corresponding composites for reanalysis data will be analyzed to establish whether the circulatory response is similar to the models' and therefore whether the modeled response is trustworthy. The implications of these findings will be discussed in the final section.

2. Model Data

Five GCM simulations are analyzed in this paper. These simulations were taken from a 17-member perturbed physics ensemble (PPE) of the Hadley Centre Coupled Model, version 3 (HadCM3) [*Murphy et al*., 2007]. HadCM3 has an atmospheric grid spacing of 2.5° latitude and 3.75° longitude and 19 vertical levels coupled to a fully dynamical ocean. The 17 versions of HadCM3 in the ensemble each have a different set of parameter values. Parameters which are poorly constrained in the model's representation of key atmospheric and land surface processes were perturbed, with the values chosen from ranges considered plausible following an expert elicitation process [*Collins et al*., 2011].

Five of these ensemble members were selected to run regional climate model experiments by *Buontempo et al*. [2014]. The subselection methodology was developed by *McSweeney et al*. [2012] and was designed to (a) eliminate model versions with a poor simulation of key features of African climate and (b) capture the range of African temperature and precipitation projections. One of the five versions chosen has the standard parameterizations of HadCM3 [*Pope et al*., 2000] and is identical to the version which has been widely used as part of the Coupled Model Intercomparison Project phase 3 (CMIP3), except for an interactive sulfur cycle, and the addition of flux adjustments included at the sea surface to ensure that baseline sea surface temperatures (SSTs) and sea ice are close to observed.

The five GCMs were run in experiments forced with historical emissions and the Special Report on Emissions Scenarios (SRES) A1B scenario from 1949 to 2100. The output was used as boundary conditions for RCM simulations using the Hadley Centre Regional Model, version 3 (HadRM3P) [*Jones et al*., 2004]: the same model used for the PRECIS regional climate modeling system. The RCM was run over the Coordinated Regional Downscaling Experiment (CORDEX) Africa domain [*Giorgi et al*., 2009] at a grid spacing of 50 km, with 19 vertical levels, and the land surface scheme MOSES 2.2 (Met Office Surface Exchange Scheme version 2.2). The core physics of the GCM and RCM is broadly similar. The RCM physics is based on the atmospheric component of HadCM3 (HadAM3), but with some structural changes to the representation of clouds, and other parameters optimized to deliver improved model performance over land regions when run as a global atmospheric model at double the standard atmospheric resolution of HadAM3/HadCM3. Details are provided in *Jones et al*. [2004] and *Massey et al*. [2014]. Throughout the paper the RCM data are analyzed at the GCM grid spacing to allow for fair comparison between GCM and RCM (but all conclusions have been tested by repeating the analysis at native resolution).

3. Future Drying Signal

In this section we examine the models' future precipitation projections over West Africa during the core of the West African monsoon (WAM) season (JAS) and explore circulation changes associated with these responses. Future changes were calculated on a grid point-by-grid point basis: the difference between the end of the twentieth century (1980–1999) and three 20 year time slices during the 21st century (2019–2038, 2049–2068, and 2079–2098), for precipitation, temperature (T), specific humidity (q), wind (V), horizontal moisture flux (qV), vertical velocity (ω), sea level pressure (SLP), and cloud. First, changes in precipitation are examined; then cross sections of ω and meridional wind (v) are inspected, since the meridional circulation in West Africa exerts an important influence on precipitation. Finally, maps illustrating anomalies in key atmospheric variables across the African continent are analyzed, to give an insight into the spatial patterns of circulation change.

3.1. Precipitation Projections

The dominant future precipitation responses in the GCM and RCM ensembles are displayed in Figures 1a and 1b, respectively. The mean of all five model versions is shown, with the level of model agreement in the direction of change illustrated using stippling for grid points where all ensemble members agree and a white mask where fewer than four models agree. Areas where the models consistently project no significant change relative to interannual variability are shown in grey: identified using a Mann-Whitney U-test of difference between the baseline and future climatologies for each model. A nonparametric test was chosen to accommodate skewed precipitation distributions in arid regions. Figure 1c displays the difference between GCM and RCM projections, but only for grid points where the direction of this difference is consistent for the majority of the five ensemble members.

Figure 1 shows large negative anomalies in western Africa in the GCMs. The magnitude of the negative anomalies increases through the 21st century and by the 2080s–2090s is >2 mm d^{-1} in the ensemble mean in west Sahel, with all GCMs showing a dry signal throughout west Sahel, the west of the Sahara, the Guinea Coast, and west equatorial Africa. The RCMs show a similar pattern of change; although, as illustrated in Figure 1c, the dry signal is weaker and is less spatially extensive, largely restricted to west Sahel and the west of the Congo Basin.

Drying in west Sahel could have serious implications [*Tarhule*, 2007], particularly at the magnitude shown by the GCMs. Understanding why this drying occurs could potentially lead to an assessment of its plausibility, and comparison between the GCM and RCM dynamics might help to ascertain whether either the larger or the more moderate drying can be considered more credible. Therefore, circulation changes concurrent with the drying response will now be examined, as a first step toward inferring mechanisms for drying in these models.

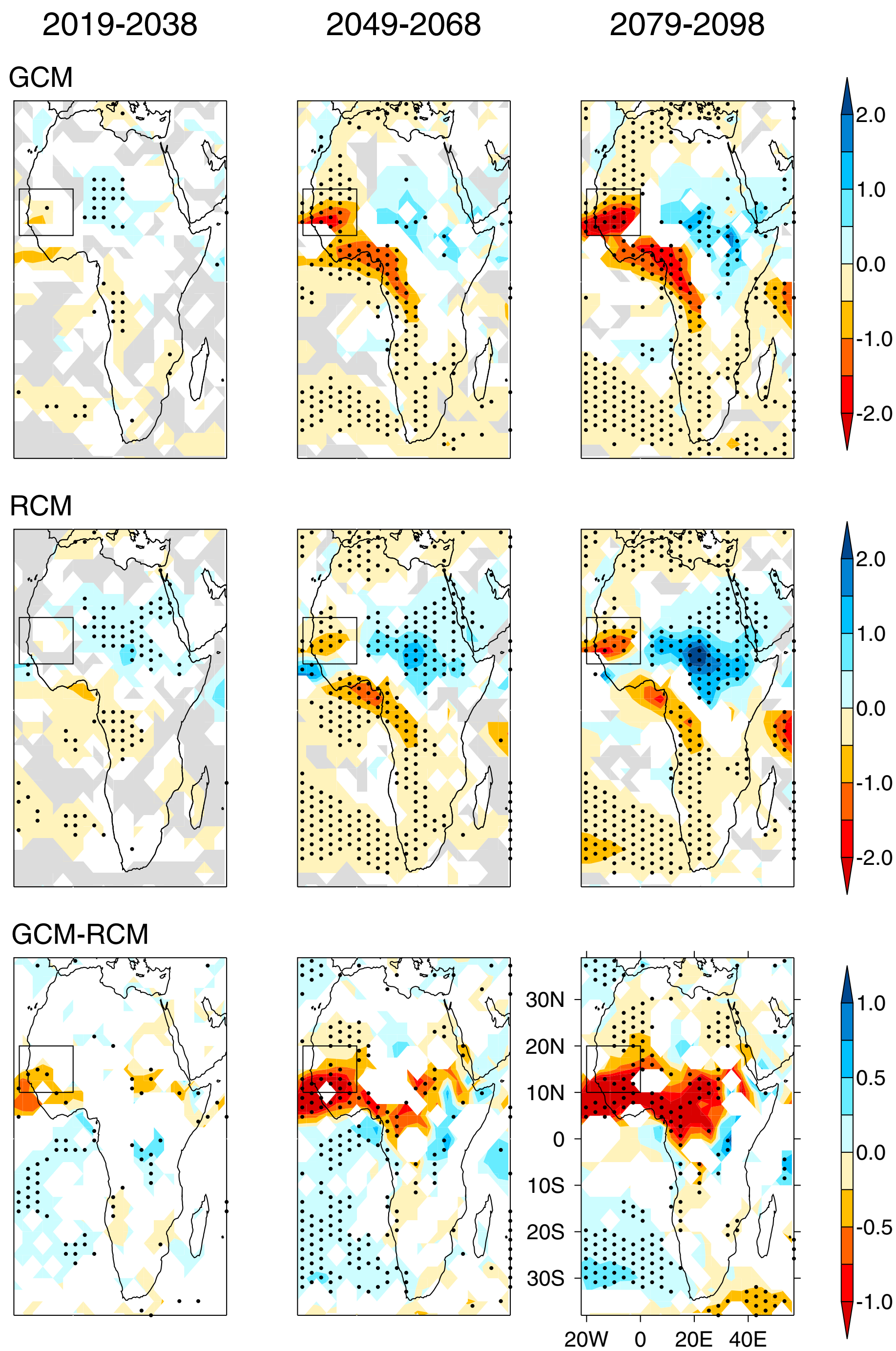

Figure 1. Projected changes in JAS precipitation (mm d^{-1}) for the early, mid, and late 21st century, for (a) GCM and (b) RCM ensemble means and (c) the difference (GCM − RCM). In Figures 1a and 1b grid points where <4(5) models agree on the direction of change are white (stippled), and grid points where none of the models experience significant change (5% level) are grey. Analysis on RCMs was conducted at the GCM resolution (analysis at native resolution leads to the same findings). In Figure 1c white (stippled) areas indicated that <4(5) models agree in the direction of difference between GCM and RCM. The black box on each map demarcates the domain used for composites in section 4.

3.2. Changes in Meridional Circulation

Zonal mean wind circulation was inspected over the core region (10°W to 0) of negative precipitation anomalies in West Africa, including west Sahel and the west of the Guinea Coast (Figure 2), and is presented in latitude-height cross sections in Figure 3 (following *Cook and Vizy* [2006]). These plots show the GCM

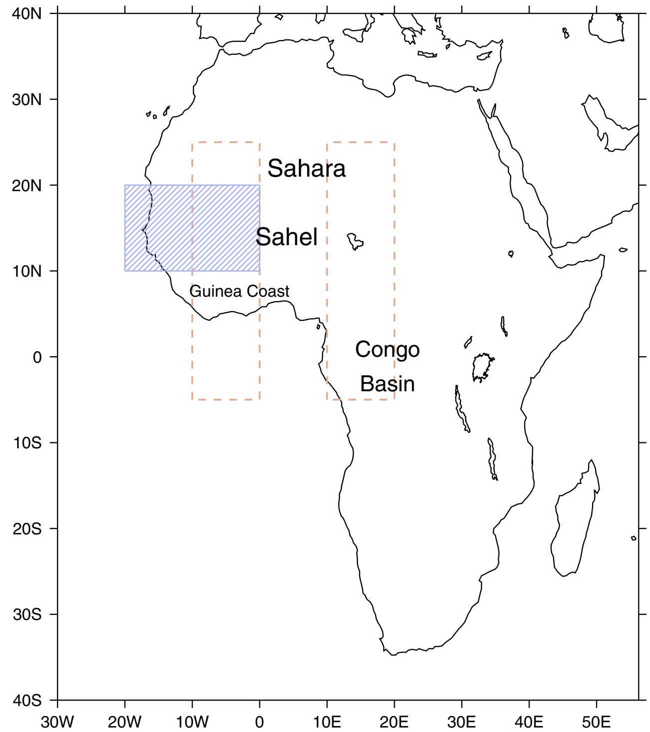

Figure 2. A map to illustrate key regions referred to in the paper and the domains used for area averaging. The dashed brown lines mark the 10°W to 0 cross section used for Figures 3, 4, and 7 and the corresponding 10–20°E cross section used in Figure S2 in the supporting information. The blue box shows the domain used for the composite analysis in section 4.

and RCM ensemble means: corresponding plots for individual models are similar (not shown). The late twentieth century climatologies of the models show monsoon inflow near the surface at the Guinea Coast (approximately 5°N), which penetrates to 20°N, and feeds ascent across these latitudes, only constrained by the anticyclonic circulation of the Saharan high, which produces subsidence in the upper troposphere (200–500 hPa) from 19°N in the GCM ensemble mean. This subsidence is more extensive in the RCMs, meaning ascent is confined to slightly lower altitudes and latitudes. Both ensembles show southward flow at 250 hPa over the Guinea Coast and subsidence above the Gulf of Guinea.

As the simulations progress through the 21st century, the Saharan high migrates southward. There is an increase in subsidence over the Sahara and northern Sahel. The monsoon circulation at the Guinea Coast moves north, allowing the subsidence over the Gulf of Guinea to spread to approximately 4°N and reducing ascent in the southern Sahel; as seen in Figure 4, which displays downward ω anomalies at all altitudes over the Guinea Coast and southern Sahel, and in the upper atmosphere further north. There is a corresponding weakening of the southward outflow from the Sahelian uplift, at 250 hPa, which may be associated with a reduction in the strength of tropical easterly jet. Near the surface, the monsoon flow is strengthened from the 2050s/2060s, as is ascent in the northern Sahel up to approximately 600 hPa, at which height it meets anomalous subsidence from the strengthened Saharan high and is diverted southward, reinforcing downward anomalies near 10°N. These dynamical changes develop progressively through the 21st century and are broadly similar between the GCMs and the RCMs.

3.3. Spatial Patterns of Change

Projected changes in ω, qV, q, and T across the African continent are shown in Figure 5. As in Figure 1 the ensemble means are shown but with masks to indicate regions where there is a lack of significance or lack of agreement between models. Maps of ω at 400 hPa substantiate findings from Figure 4 of downward anomalies in the upper atmosphere. For each ensemble the spatial pattern of change closely matches the precipitation anomalies in Figure 1, with downward anomalies in west Sahel, the Guinea Coast, and the Congo Basin. In the GCMs this signal has a particularly large spatial extent and a magnitude of $>1.6\,\text{hPa s}^{-1}$ in the ensemble mean by the 2080s/2090s. In north central Sahel both ensembles show smaller upward anomalies (approximately $0.8\,\text{hPa s}^{-1}$) corresponding to the wet signal in Figure 1. These changes are amplified through the 21st century. This suggests a strong association between ω at 400 hPa and simulated precipitation.

There are also downward anomalies at lower levels in the Congo Basin (to 700 hPa) and the Guinea Coast (to 850 hPa) (see Figure S1 in the supporting information), but in the north west Sahel the maps show an increase in uplift in the low to middle troposphere, in keeping with Figure 4. This anomalous ascent increases in amplitude and spatial extent through the 21st century and has a stronger signal in the GCMs than in the

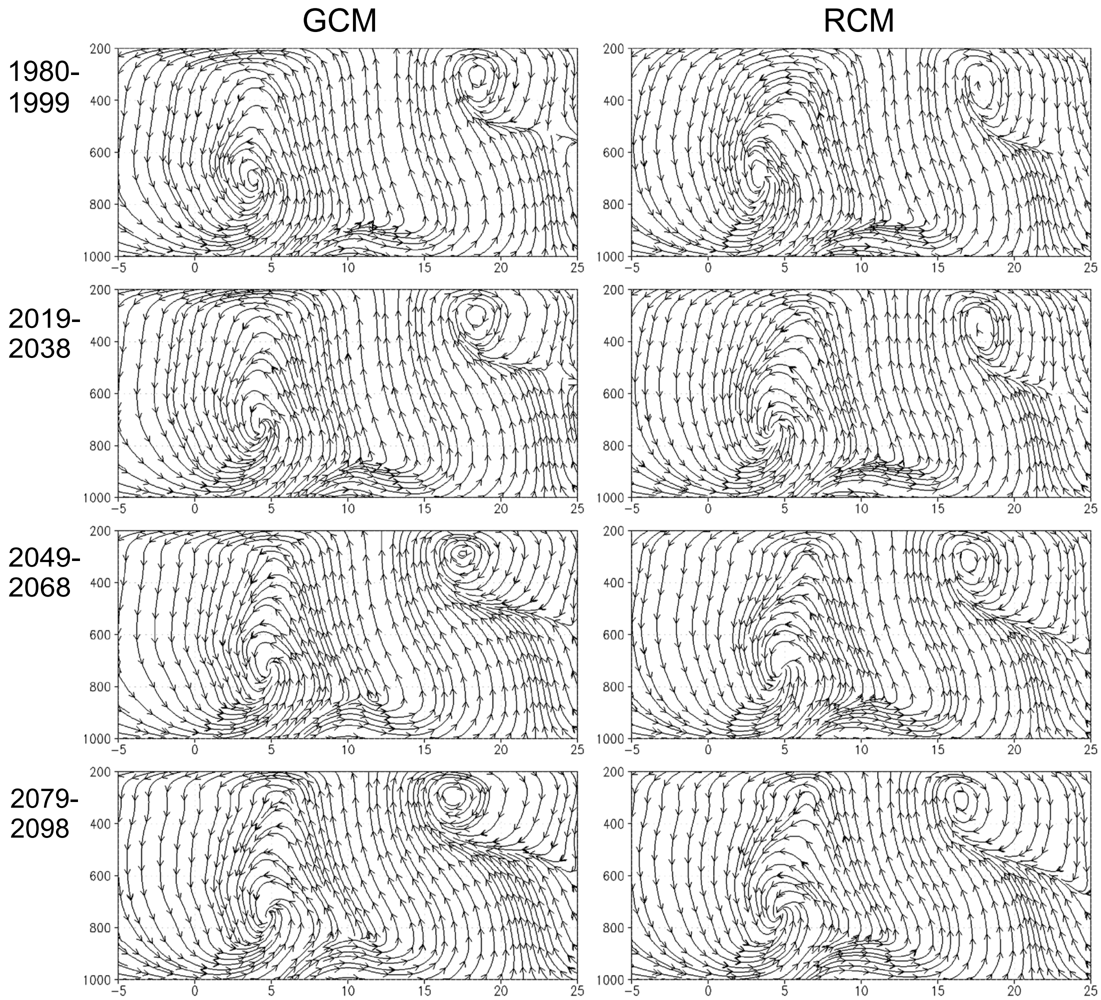

Figure 3. Latitude-height cross sections of streamlines (v ; $-\omega$*100) averaged 10°W to 0 (see Figure 2) during JAS, for the GCM and RCM ensemble means, in the twentieth century reference period and for the 21st century time slices. For clarity, the RCM is plotted at GCM resolution (equivalent figures at native resolution produce the same findings).

RCMs. The *qV* maps demonstrate that the increased northward wind flow noted in the meridional cross sections is part of a large-scale amplification or northward shift of the monsoon circulation, with an increase in moisture flux from the Atlantic and the Guinea Coast (where there is divergence) to the northern Sahel (where there is convergence). This moisture convergence is at approximately 18°N in west Sahel and slightly further north (22°N) in central and east Sahel in both ensembles.

3.4. Hypothesized Mechanisms for Drying

This paper does not aim to say exactly why the dry signal occurs, since this is not possible using output from future simulations: idealized experiments would be needed to establish causality. However, through analysis of circulation changes which coincide with precipitation change, we can make hypotheses about the mechanisms for drying. Given the similarity of the response between the GCMs and the RCMs, the difference between them appears to be only in magnitude and not in the characteristics of the changes (see Figure 5c). We therefore assume that the smaller precipitation anomalies in the RCMs are not due to different atmospheric dynamics but a weaker version of the same mechanism.

The mechanism for drying is not immediately obvious: the amplification of the monsoon flow, increase in moisture convergence, and enhanced uplift found near the surface of west Sahel may seem to contradict the strong precipitation decline. Many previous studies have postulated that a strengthening of the WAM would be a plausible response to global warming, due to changes in interhemispheric SST

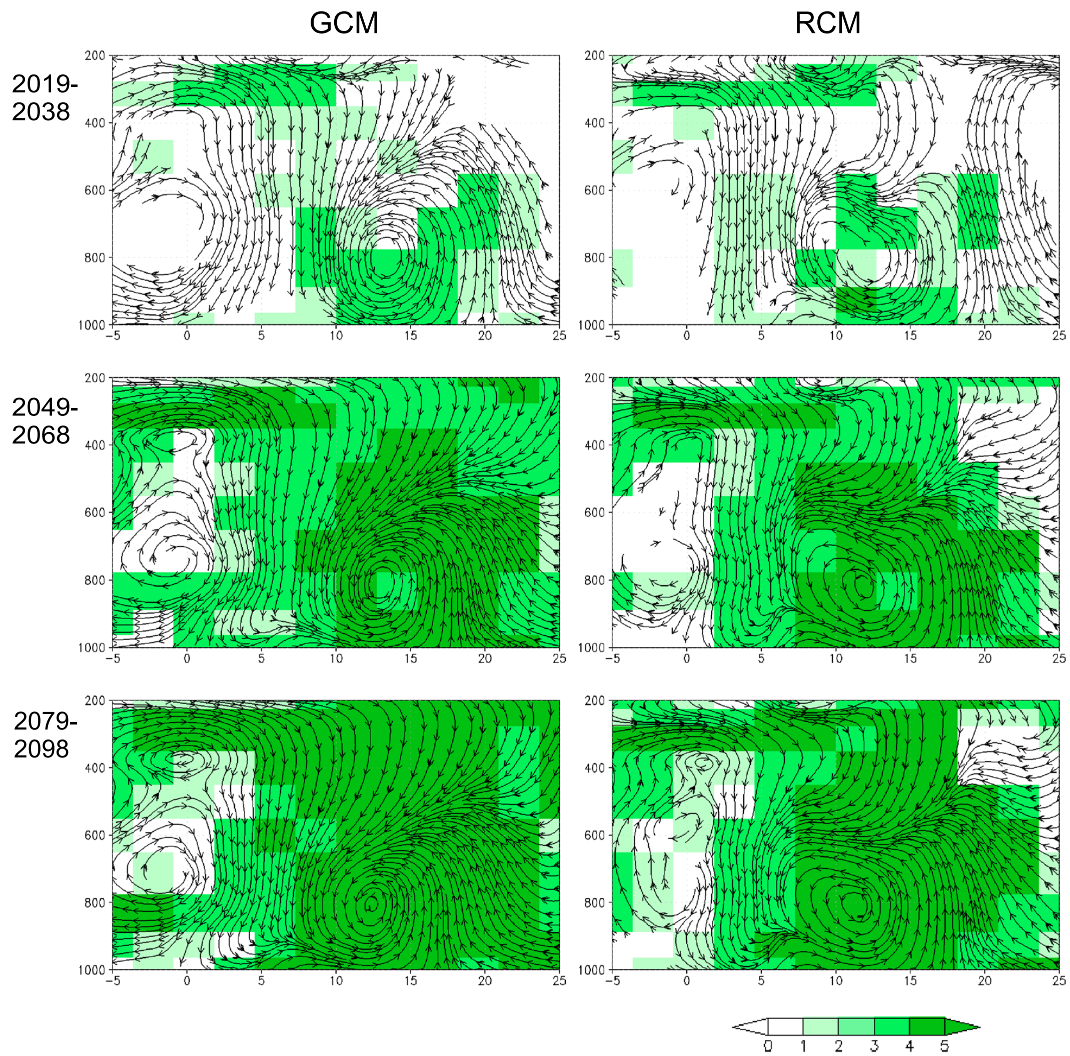

Figure 4. Same as Figure 3 but for anomalous streamlines associated with each 21st century time slice. Green shading indicates the number of models which show significant change (in either *v* or ω) of the same direction (5% level).

gradients [e.g., *Hoerling et al*., 2006], an increase in the land-ocean temperature contrast [*Haarsma et al*., 2005], or a deepening of the Saharan heat low (SHL) [*Biasutti et al*., 2009]. This is expected to lead to wetter conditions in the Sahel. The strengthening of the monsoon circulation found in the GCMs and RCMs used here may be responsible for the wetting in central and east Sahel. It might also explain the drying at the Guinea Coast and the Congo Basin: the dipole between the Guinea Coast and the Sahel caused by a northward shift in the monsoon circulation is well known [e.g., *Vizy and Cook*, 2002], and some also relate precipitation in Central Africa to latitudinal changes in tropical convection [e.g., *Tokinaga and Xie*, 2011].

In west Sahel, however, there is no corresponding increase in precipitation, but rather some of the largest negative anomalies experienced anywhere on the continent. This is likely due to the ω changes aloft, which cap the anomalous uplift from the surface at approximately 500 hPa; in contrast to central Sahel, where there are upward anomalies throughout the atmospheric column (Figure S2 in the supporting information). It is worth noting that, despite the general increase in atmospheric moisture content in response to global warming [*Allen and Ingram*, 2002], *q* does not increase in west Sahel in the GCMs (Figure 5). Therefore, while there is anomalous uplift at the surface of the north western Sahel, it is not an increase in moist convection: lapse rates of potential temperature between the surface and 600 hPa decrease in future (not shown), suggesting that convection becomes drier.

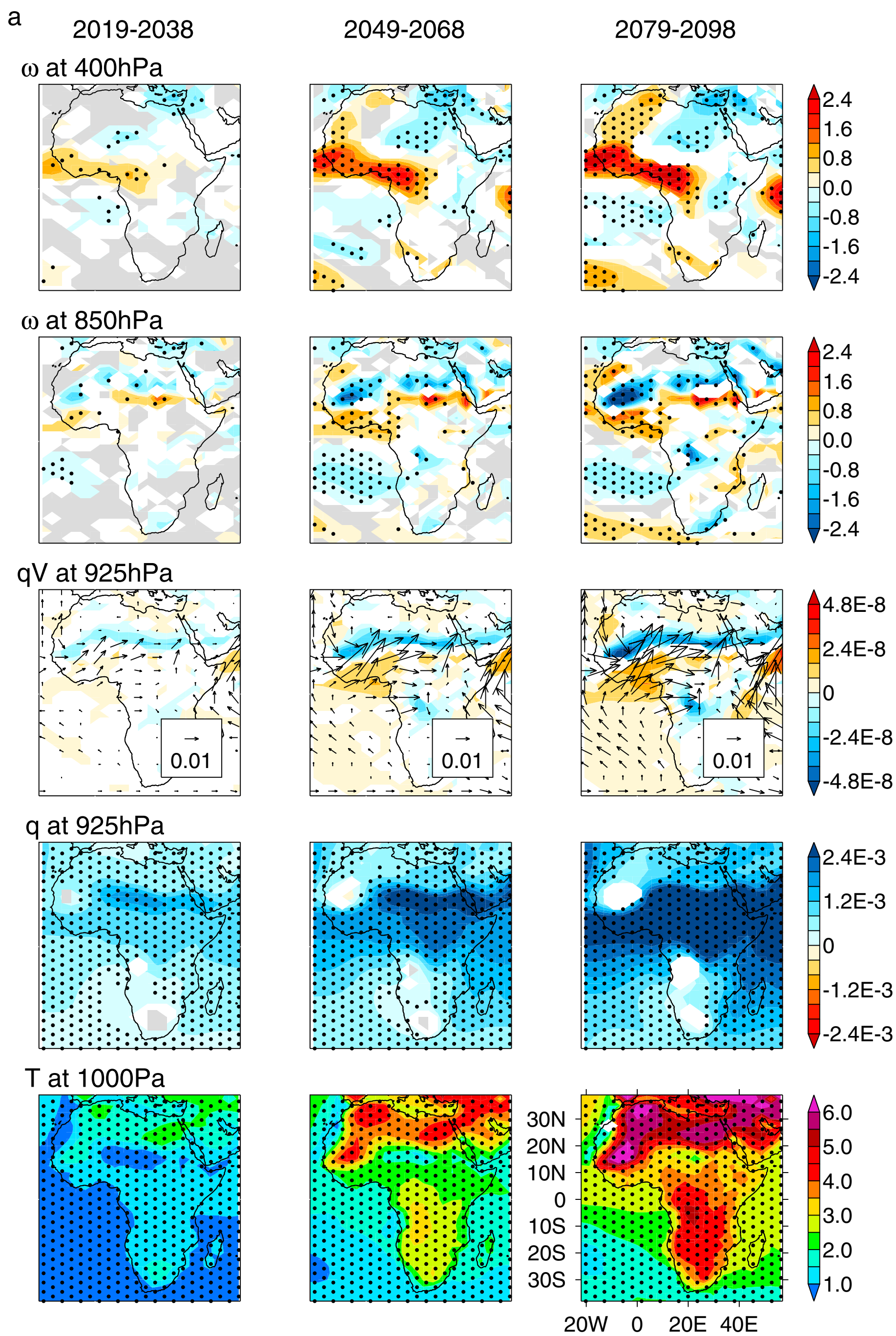

Figure 5. Future projections during JAS for ω at 400 hPa and 850 hPa (hPa s^{-1}), qV at 925 hPa (kg kg^{-1} ms^{-1}) with contours of moisture divergence (kg kg^{-1} s^{-1}), q at 925 hPa (kg kg^{-1}), and temperature at 1000 hPa (°C) in (a) GCM and (b) RCM ensemble means and (c) the difference (GCM − RCM). For all variables except qV significance and intermodel agreement is shown as in Figure 1. For qV and contours of divergence, in Figures 5a and 5b white areas indicate that <4 models agree in the direction of change or all models show no significant change, and in Figure 5c white areas indicated that <4 of models agree in the direction of difference between GCM and RCM. Analysis on RCMs was conducted at the GCM resolution (analysis at native resolution leads to the same findings).

The zonal contrast in ω anomalies, possibly remotely forced, therefore appears to explain the drying in west Sahel despite the increase in the monsoon flow. Previously, many CMIP3 [*Monerie et al.*, 2012b] and CMIP5 [*Monerie et al.*, 2012a] models have also been shown to exhibit a strengthened monsoon flow but precipitation decline in west Sahel in association with downward anomalies. It is conceivable that drying of

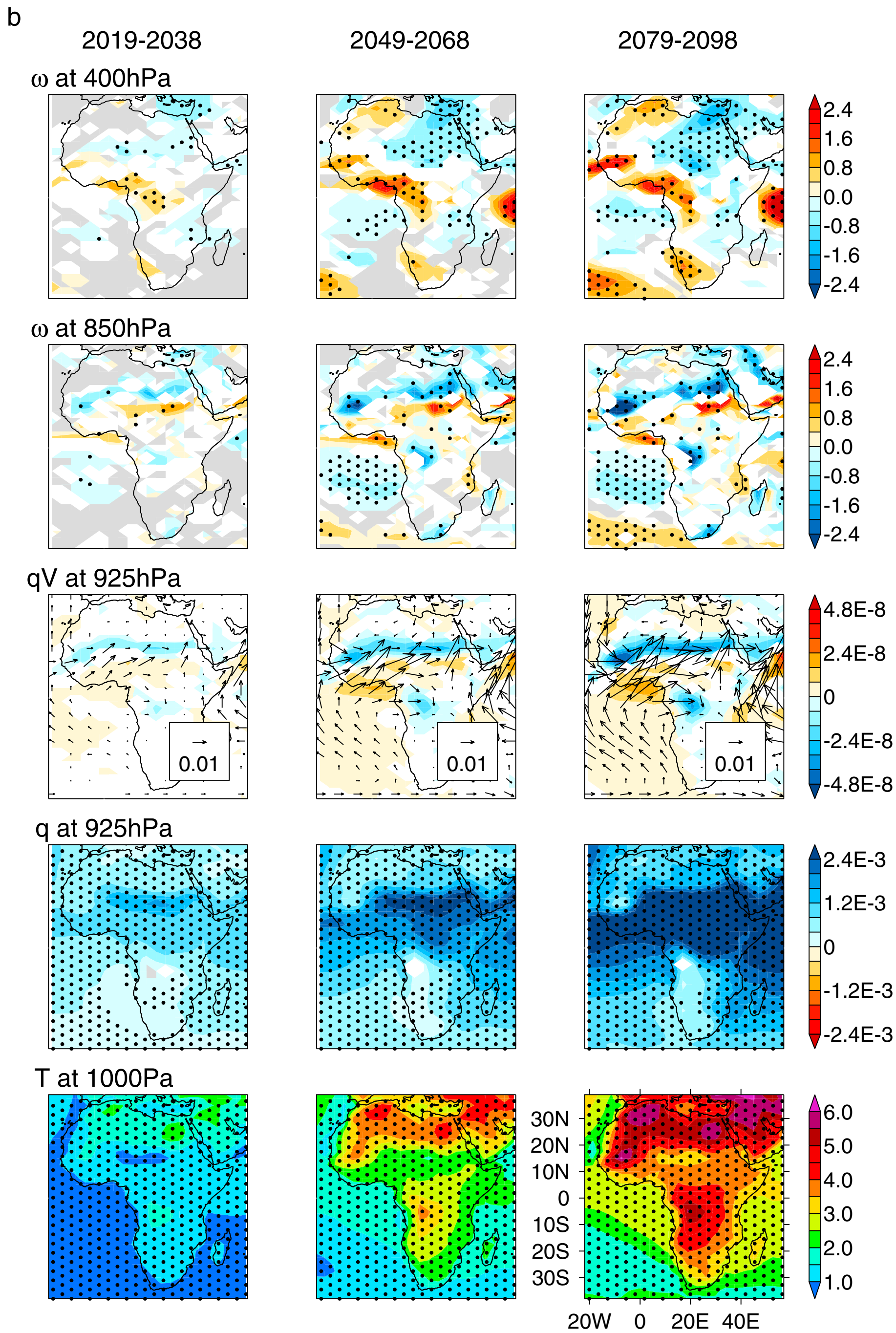

Figure 5. (continued)

west Sahel could have feedback effects which strengthen the monsoon. Both GCMs and RCMs project an associated reduction in cloud (not shown) and large temperature anomalies at the surface of the west Sahel and west Sahara (>5 °C during the 2080s/2090s; Figure 5) relative to the rest of Africa and the surrounding oceans. SLP consequently decreases (not shown), suggesting a strengthening of the SHL, which could act to enhance the WAM. This possibility complicates the relationship between the heat low and precipitation presented by *Biasutti et al*. [2009], who find that a stronger SHL leads to a wetter Sahel. The role of the SHL may be contingent on the location of maximum warming, as implied by *Vizy et al*. [2013].

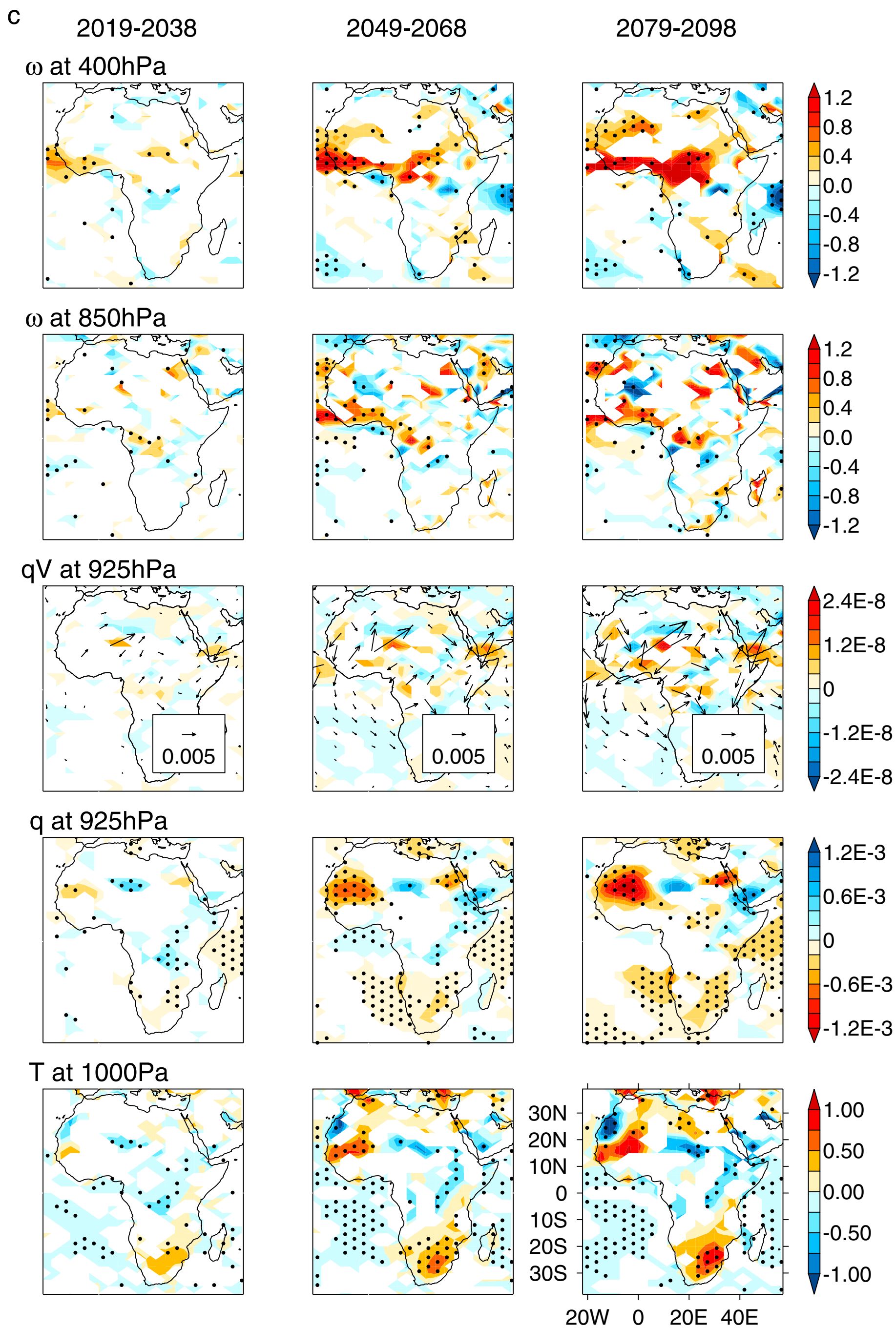

Figure 5. (continued)

As well as influencing the monsoon, the heat low region has an influence on the African easterly jet (AEJ). As west Sahel becomes drier in the models, there is an increase in temperature, decrease in humidity, and decrease in pressure relative to the Guinea Coast (Figure 5). Strengthening and southward migration of these gradients (not shown) may be responsible for the increase and southward shift of the AEJ, which is found in the *qV* anomalies at 700 hPa and 600 hPa (Figure S3 in the supporting information) and the southward anomalies at these levels in Figure 4. Many authors have linked changes in the AEJ to Sahel precipitation [e.g., *Jenkins et al.*, 2005; *Sylla et al.*, 2010]: it may have a feedback effect via the influence on the African easterly waves [*Nicholson and Grist*, 2003] and through moisture export to the Atlantic. So while the uplift in

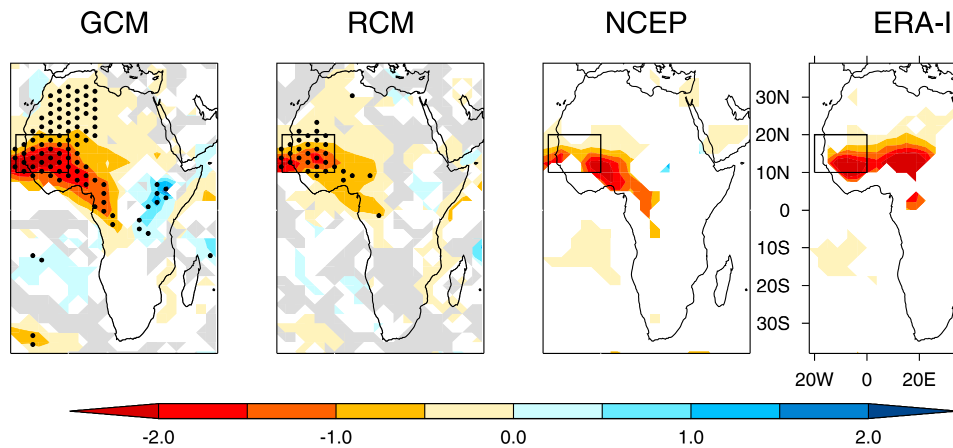

Figure 6. Dry minus wet composite JAS precipitation (mm d^{-1}) for GCM and RCM ensemble means, NCEP, and ERA-I. For reanalysis, only areas where the difference between dry and wet composites is significant relative to variation between years are shown (5% level). For model ensembles, areas where <4 (all 5) models agree in the direction of difference between dry and wet years are white (stippled), and grey indicates that all models show no significant difference between dry and wet composites relative to variation between years (5% level). All data sets have been analysed at GCM grid spacing (analysis at native resolution leads to the same findings). The black box on each map demarcates the domain used for the composites.

northern Sahel may not be expected together with negative precipitation anomalies, it could, in fact, be a response to drying and pronounced warming, which may be associated with feedback effects via the WAM and/or AEJ.

Elucidating these mechanisms could require substantial further work. Yet having described the circulatory response, we can already begin to assess whether this is credible, and this is the focus of the next section.

4. Historical Wet and Dry Years

It is impossible to validate future changes in atmospheric dynamics, so instead dry years in the models' historical simulations will be examined. If the modeled circulation anomalies during these dry years are similar to those associated with future drying, then the modeled dry years can be compared to observed dry years to assess the reliability of the future response.

Given the limited availability of observations in West Africa, here results from the GCM and RCM ensembles will be presented alongside reanalysis data, from two of the most widely used products: National Centers for Environmental Prediction (NCEP)-National Center for Atmospheric Research reanalysis 1 (NCEP) [*Kalnay et al.*, 1996] and ERA-interim (ERA-I) [*Dee et al.*, 2011]. While these data sets have been found to exhibit large biases in the water budget over West Africa, reanalysis products are still a reasonable tool, and indeed the only one available, for examining interannual variations in atmospheric circulation in this region [*Meynadier et al.*, 2010].

Composite analysis was conducted for the models and reanalyses, focusing on the region with the largest negative precipitation anomalies in Figure 1: "West Sahel" (20 W–0; 10–20 N) (following *Hastenrath* [2000]). The 10 wettest and 10 driest years in West Sahel in JAS were selected from precipitation time series for the two reanalysis data sets (1979–2009, due to availability of ERA-I) and each model (1979–2009; note that results for 1960–1999 are the same). The difference between dry and wet composites (dry − wet) was calculated for a range of atmospheric variables and tested for significance relative to variation between years using the Mann-Whitney *U*-test. For all data sets the tests were computed at native resolution and at the GCM grid spacing to allow for fair comparison.

The spatial signatures of the precipitation composites are presented in Figure 6 to provide a context for the investigation of atmospheric dynamics. During dry years in West Sahel the GCMs and RCMs also experience drying over parts of the west Sahara, the Guinea Coast, the west of the Congo Basin, and, in most models, the central Sahel. This is very similar to the spatial pattern of change in their precipitation projections

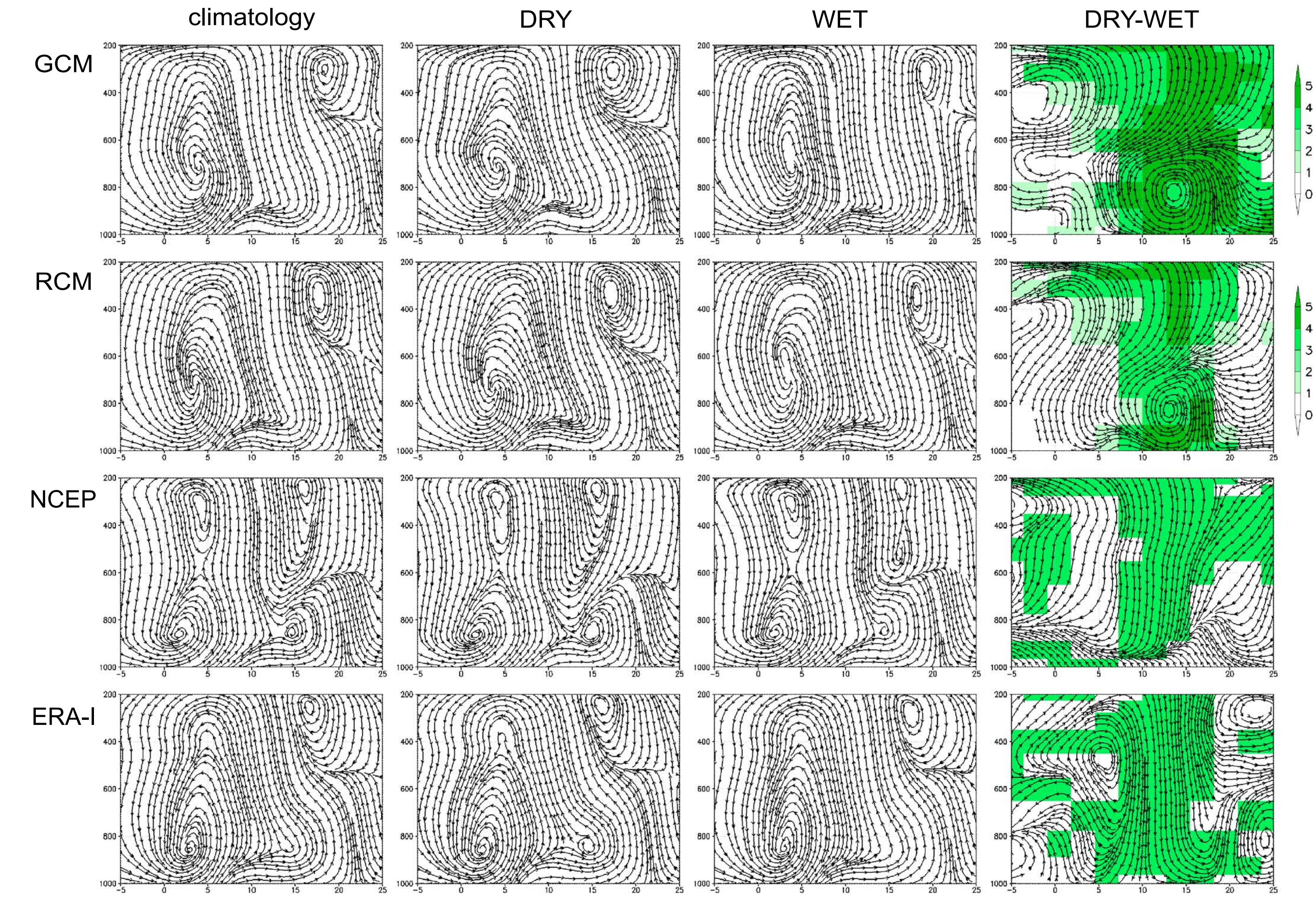

Figure 7. Latitude-height cross sections of streamlines (v; $-\omega$*100) averaged 10°W to 0 (see Figure 2) during JAS, for the long-term mean (1979–2009), dry, wet, and dry minus wet composites, for GCM and RCM ensemble means, NCEP, and ERA-I. For reanalysis, the green shading on the dry-wet plots indicates significant difference between dry and wet composites (in either v or ω) relative to variation between years within the composites. For the model ensembles, the green shading indicates the number of models which show significant difference between dry and wet composites (in either v or ω) of the same direction (5% level). All data sets are plotted at the horizontal and vertical resolution of the GCM. Equivalent figures at native resolution are provided as Figure S5 in the supporting information.

(Figure 1) (with the exception of central Sahel), suggesting that the composites are a useful means of appraising the dry signal associated with global warming. The precipitation maps for the reanalyses are different (Figure 6). The largest anomalies are in central Sahel, to the south of the Sahel, and in parts of central Africa, rather than in West Sahel. This suggests a difference in modes of interannual variability between the models and reanalysis, which is now explored further through meridional circulation anomalies and spatial patterns of change in selected atmospheric variables.

4.1. Meridional Circulation Anomalies

Before examining the dynamics associated with dry years, the long-term mean circulation in each data set is inspected (Figure 7). The model ensembles show almost identical flow as for the 1980–1999 mean in Figure 3, described in section 3.2. While they have a relatively good representation of the meridional circulation in comparison to some CMIP3 models [see *Cook and Vizy*, 2006], there are important differences from the reanalyses.

In both the GCMs and the RCMs there is uplift from approximately 5°N to the Sahara, with little subsidence aloft to prevent uplift, whereas NCEP shows two distinct zones of convergence, with deep moist convection between 5 and 10°N and a shallower region of dry convection associated with the thermal low in the southern Sahara. In between these two zones upward motion is restricted to higher levels (above approximately 600 hPa) and the monsoon flow at the surface is vertically confined by southward and downward motion at 800 hPa. The ERA-I plot is more similar to the models', but the equivalent figures at native resolution (Figure S4 in the supporting information) demonstrate that this data set also shows convection to be restricted in the northern Sahel by southward flow at 700 hPa.

In all data sets, the uplift in the Sahara is capped by subsidence from the Saharan high, but this occurs at lower levels and lower latitudes in the reanalyses relative to the RCMs and especially the GCMs; meaning the models do not show the southward outflow from the Saharan high at 600 hPa, which is associated with the AEJ. Note that there are also important differences between ERA-I and NCEP: prominently, NCEP shows sinking air to 900 hPa at 12°N, which is not found in ERA-I.

Given the differences in background climatology we might also expect differences between data sets in the dynamics associated with dry and wet years. The model ensembles' response in dry years is very similar to their future response: the dry-wet composites in Figure 7 correspond closely to the anomaly plots in Figure 4 (see Figure S5 in the supporting information for a direct comparison). Note that anomalies to the long-term mean for many individual dry years (not shown) also exhibit this mode: with downward anomalies above 500 hPa from 5°N to the Sahara, and the same anomalous overturning nearer the surface, with an increase in monsoon flow, uplift in northern Sahel, southward motion at 600 hPa, and downward anomalies in southern Sahel.

The reanalyses show different dynamics from the models. The main distinction between dry and wet composites is in the amount of convection over the Sahel. The dry-wet composites show significant downward anomalies from just above the surface to 200 hPa and from approximately 8–15°N in both NCEP and ERA-I. There are also differences between the reanalysis products. They each share some but not all of the features shown by the models. ERA-I, like the GCMs and RCMs, suggests that the Saharan high moves further south in dry years and has significant upward anomalies near the surface of the northern Sahel/southern Sahara, although these are further north than in the RCM. NCEP also has an increase in convection at the surface of the northern Sahel, but it is confined to lower levels (800 hPa) than in the models and ERA-I (600 hPa).

4.2. Spatial Anomaly Patterns

The meridional cross sections suggest that the GCMs and RCMs have similar dynamical responses in future as during historical dry years. The spatial patterns of change in Figure 8 support this finding. As during the 2080s/2090s, the anomalies associated with dry (minus wet) years include subsidence at 400 hPa ($>$1.5 hPa s^{-1} over much of west Africa in the GCM and RCM ensemble means) and large warming near the surface of west Sahel ($>$2 °C in the GCM mean). In both the GCMs and the RCMs there is uplift in low levels of the northern Sahel, but also a decrease in q, suggesting this is dryer convection than in wet years (which is confirmed by lapse rates of potential temperature; not shown). This dry convection meets the subsidence aloft and is diverted south, as shown in southward anomalies of qV at 600 hPa, which are associated with large-scale moisture divergence in West Africa (Figure S9 in the supporting information) and subsidence over the Guinea Coast.

Near the surface there is moisture flux from southern to northern West Africa and moisture convergence in northern Sahel. However, this is not associated with a large-scale increase in the monsoon circulation as in future. In fact, qV anomalies at 925 hPa in the Atlantic suggest a weakening of the monsoon flow. This may explain the different sign of anomalies in the central Sahel. Another difference in qV between the dry-wet composites and the future anomalies is in the low-level westerlies (LLWs) from the Atlantic at 850 hPa (Figures S3 and S9 in the supporting information), which decrease (increase) in dry years (future). The composites therefore imply that decreases in LLWs and a reduction in the monsoon circulation are associated with drying, as would be expected from previous literature [e.g., *Nicholson*, 2009; *Sylla et al*., 2010], but this does not fit with the models' future response. It could be that other drivers, for example subsidence in the upper troposphere, are sufficient to cause drying in the future simulation *despite* increases in the WAM and LLWs. Or it might be that the drying in future, when combined with global warming, leads to a larger magnitude temperature increase in west Sahel and North Africa, and the increased land-sea contrast *forces* an increase in the WAM and LLWs.

There are thus some aspects of the dynamics associated with the future drying trend which cannot be appraised based on the composites. The circulation anomalies nevertheless show sufficient similarity

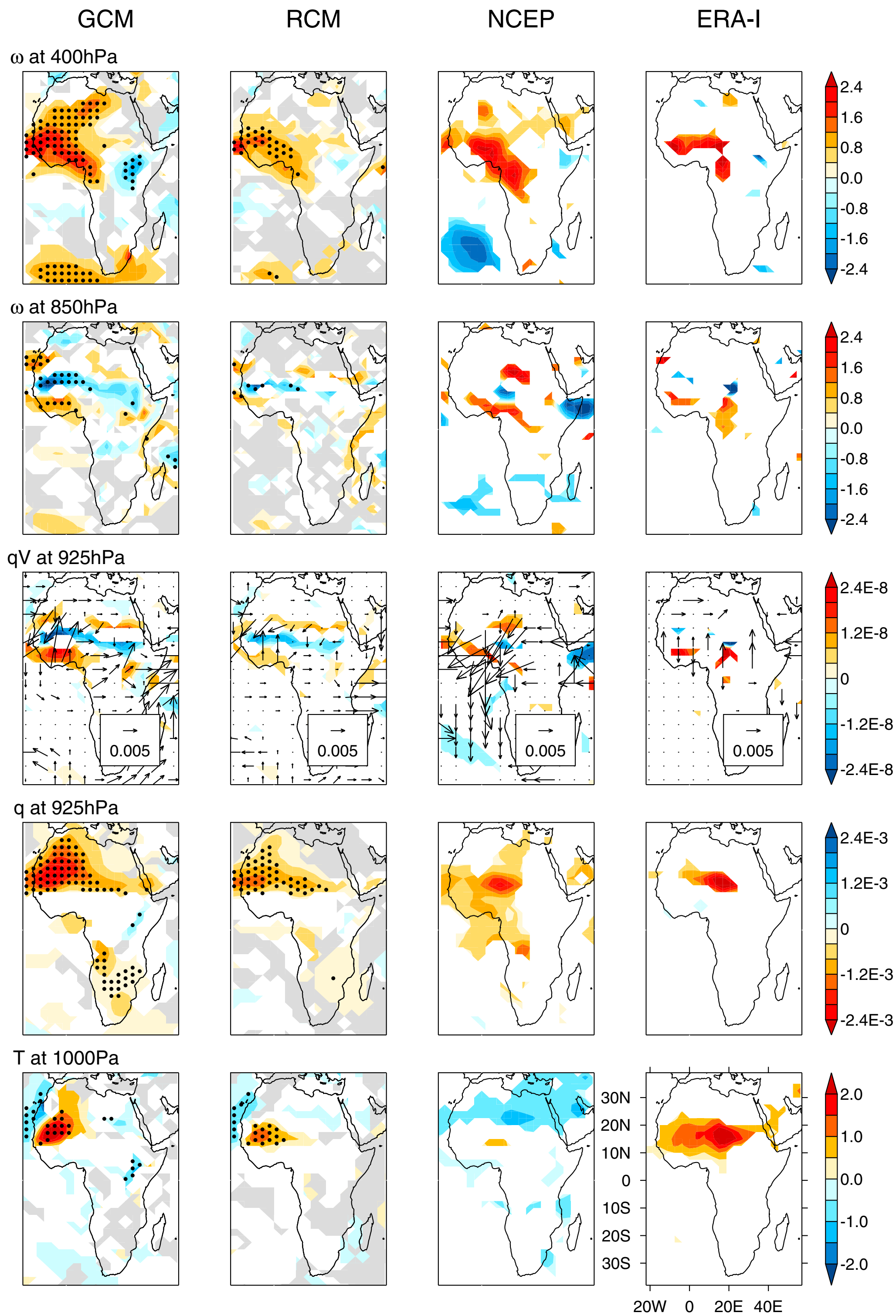

Figure 8. Dry minus wet JAS composites for ω at 400 hPa and 850 hPa (hPa s^{-1}), qV at 925 hPa (kg kg^{-1} ms^{-1}) with contours of moisture divergence (kg kg^{-1} s^{-1}), q at 925 hPa (kg kg^{-1}), and temperature at 1000 hPa (°C), for GCM and RCM ensemble means, NCEP, and ERA-I. For all variables except qV for models, significance and intermodel agreement is shown as in Figure 6. For qV and contours of divergence in models, white areas indicate that $<$4/5 models that agree in the direction of difference between composites or all models show no significant difference. The same figure with no significance testing is provided in Figure S7 in the supporting information, and dry and wet composites are provided in Figure S8. All data sets have been analyzed at GCM resolution (analysis at native resolution leads to the same findings).

between composite and future simulation to imply that the main responses associated with drying are consistent. And while some of these are shared by the reanalysis, other elements are distinct. All of the data sets show close correspondence between precipitation anomalies and ω at 600–400 hPa (Figures 8 and S8 in the supporting information). There are also easterly anomalies in all data sets near the Guinea Coast at 700–600 hPa (Figure S9 in the supporting information), implying a strengthening of the AEJ; and, as noted from the meridional cross sections, both NCEP and ERA-I show some upward anomalies at 850 hPa in the Sahel, possibly representing a more muted version of the stronger increase in ascent in the models. Both of these changes are likely responses to rather than causes of drying but, as discussed in section 3.4, may have feedback effects. Given the much larger amplitude in the models (particularly the GCMs), any feedback effects would be exaggerated in comparison to the reanalyses.

The magnitude of drying in the reanalyses would seem to be derived not from feedbacks but from larger forcings. In NCEP there are large qV anomalies at 925 hPa, which show north easterly moisture flux from the central Sahel to the Atlantic, indicating a weakening of the WAM, which is not matched by the models or ERA-I. And, in both NCEP and ERA-I there would appear to be strong connection with ω in the lower troposphere over west Sahel (seen in Figure 8 at 850 hPa; and for other levels, see Figure S8 in the supporting information), which is not shown by the models. Correlations between ω at 700 hPa and precipitation suggest that this is a strong relationship in both NCEP and ERA-I ($r = -0.9$ and -0.8, respectively) but not in the GCMs or RCMs. *Hastenrath* [2000] also finds that dry years in NCEP are associated with anomalous subsidence throughout the atmospheric column.

4.3. Findings From Composite Analysis

While there are some differences between modeled dry years and the modeled future responses, there appears to be a common mode, with the largest precipitation anomalies in west Sahel, downward anomalies in the upper troposphere, and possible feedback effects linked to a strong warming of the heat low region. The models generate this mode during dry years in the historical period and then appear to shift into this mode in future. The reanalyses have some points of similarity with the modeled mode, but the differences are sufficient to show that the mode is not found in the reanalyses: NCEP and ERA-I do not have a dominant response in west Sahel and appear to have additional forcings during dry years. There is no guarantee that the reanalysis accurately capture the dynamics associated with dry years, but the difference between the results from the reanalyses and the models nevertheless casts doubt on the modeled dry signal in West Sahel. Since the GCM and RCM have such similar responses, the RCM does not appear to be more credible in this case.

5. Summary and Discussion

An understanding of how climate change might affect vulnerable regions could be highly valuable; however, future projections from models have large uncertainties and often diverge in the direction as well as the magnitude of change. Decision makers need to know which of these projections they should trust. The majority of research to evaluate climate models is based on comparison of hindcasts with observed data. Yet in order to interrogate the credibility of modeled projections, it is necessary to directly assess changes as well as historical climatological means. This paper presents a methodological framework for process-based analysis of projections, applied to investigate a strong drying signal in West Africa in a group of five MOHC global and regional models. Circulation changes associated with the precipitation response are analyzed and compared to historical atmospheric dynamics using composites of wet and dry years from the models and reanalysis data sets.

The dry signal in question covers much of western Africa, including west equatorial Africa, the Guinea Coast, and the west of the Sahara, but has the highest magnitude in west Sahel, particularly in the global models, at $>2\ \text{mm d}^{-1}$ in the ensemble mean. Such a decline in precipitation would have serious implications for the Sahel, and therefore, investigating its credibility is a priority. Analysis of atmospheric circulation reveals that the drying is associated with anomalous subsidence at 400 hPa, possibly amplified by a large warming of the surface ($>5\,^{\circ}$C in the 2080s/2090s) in west Sahel and the west Sahara. This warming may be responsible for increases in dry convection in northern Sahel and a strengthening of the heat low, with potential feedbacks on the monsoon and the AEJ.

The circulatory response is common to both the global and regional models, only slightly weaker in the RCMs, which show smaller precipitation anomalies. Composite analysis suggests that a similar mode is present in the models during the driest years for West Sahel in the 20th and early 21st century. Historical composites can therefore be used to assess future drying based on comparison with reanalysis data, and here NCEP and ERA-I are employed. The modeled circulation mode is, however, not found in the reanalyses, which appear to have different mechanisms for drying in West Sahel. This casts doubt on the future drying in these models: a finding which might have important implications for the Sahel and for conducting regional climate change assessments.

5.1. Implications for the Sahel

While further work would be needed before the dry signal in these versions of HadCM3 (and HadRM3P) could be rejected; the difference between the models and reanalysis does not inspire confidence and therefore brings this strong drying into question. This does not imply that a wetter future is more likely. Many models show positive precipitation anomalies in the Sahel [*Hoerling et al*., 2006], including state-of-the-art RCM experiments [*Vizy et al*., 2013]; but there are also many others which project negative anomalies, particularly in the west of the Sahel [*Monerie et al*., 2012a; *James and Washington*, 2013]. To better understand which futures are plausible and credible, each projection deserves further analysis to investigate the mechanisms for change.

5.2. Implications for Regional Climate Change Assessments

The need for approaches to better represent climatic uncertainty in regional climate impacts assessments and adaptation planning is clear. The range of projected futures is different depending on which ensembles are used, and how they are constrained [*James et al*., 2014]. Global and regional models also have different outcomes, and RCMs do not necessarily produce more realistic futures through higher resolution. This is underlined by the results in this paper, which do not show a measureable improvement from the GCM to the RCM.

An understanding of the credibility of specific model projections could be very useful. This study provides a framework to inform confidence in projected futures, through investigation of circulation changes using composites of wet and dry years. The analysis conducted here could be extended to further test the plausibility of the drying in the MOHC models employed, for example applying idealized experiments to better understand the mechanisms for change. The framework could also be used with other models to constrain the range of projections over West Sahel.

One potential caveat is observational uncertainty in the climatological circulation and mechanisms for interannual variability. As noted above, there are biases in the reanalysis data sets used here [*Meynadier et al*., 2010], and the results in Figures 6–8 illustrate differences between NCEP and ERA-I, highlighting weaknesses in our understanding of atmospheric dynamics in this region. It would now be worthwhile to investigate whether data from short-term field campaigns can aide understanding of mechanisms for increases or decreases in precipitation, for example through comparison of wet and dry days. For West Africa data from the African Monsoon Multidisciplinary Analysis field campaigns are a potentially valuable resource. Other African regions may not be so fortunate, but if analysis for West Africa proves fruitful, this could provide yet another justification for field campaigns in previously understudied regions such as the Congo Basin [*Washington et al*., 2013].

Acknowledgments
The GCM data used in this study were produced through work supported by the UK Joint "Department for Energy and Climate Change" (DECC) and "Department for Environment, Food and Rural Affairs" (Defra) MOHC Climate Programme (GA01101). Data are available via the British Atmospheric Data Centre (http://badc.nerc.ac.uk/browse/badc/hadcm3/data/PRECIS), which is accessible after registration at http://badc.nerc.ac.uk/cgi-;bin/dataset_registration/dataset_info.cgi.pl?datasetid=link. The RCM experiments were generated by the PRECIS team at the MOHC. The authors would like to thank Carlo Buontempo, Karina Williams, and David Sexton for assistance with data access. We also acknowledge NOAA/OAR/ESRL PSD and ECMWF for making available the NCEP and ERA-I data sets.

References

Allan, R. P., and B. J. Soden (2008), Atmospheric warming and the amplification of precipitation extremes, *Science*, *321*(5895), 1481–1484, doi:10.1126/science.1160787.

Allen, M. R., and W. J. Ingram (2002), Constraints on future changes in climate and the hydrologic cycle, *Nature*, *419*(6903), 224–232, doi:10.1038/nature01092.

Biasutti, M., I. M. Held, A. H. Sobel, and A. Giannini (2008), SST forcings and Sahel rainfall variability in simulations of the twentieth and twenty-first centuries, *J. Clim.*, *21*(14), 3471–3486, doi:10.1175/2007JCLI1896.1.

Biasutti, M., A. H. Sobel, and S. J. Camargo (2009), The role of the Sahara low in summertime Sahel rainfall variability and change in the CMIP3 models, *J. Clim.*, *22*(21), 5755–5771, doi:10.1175/2009JCLI2969.1.

Buontempo, C., C. Mathison, R. Jones, K. Williams, C. Wang, and C. McSweeney (2014), An ensemble climate projection for Africa, *Clim. Dyn.*, doi:10.1007/s00382-014-2286-2.

Collins, M., B. B. B. Booth, B. B. Glen, R. H. James, D. M. H. Sexton, and M. J. Webb (2011), Climate model errors, feedbacks and forcings: A comparison of perturbed physics and multi-model ensembles, *Clim. Dyn.*, *36*, 1737–1766, doi:10.1007/s00382-010-0808-0.

Cook, K. H., and E. K. Vizy (2006), Coupled model simulations of the West African Monsoon system: Twentieth- and twenty-first-century simulations, *J. Clim.*, *19*(15), 3681–3703, doi:10.1175/JCLI3814.1.

Dee, D. P., et al. (2011), The ERA-Interim reanalysis: Configuration and performance of the data assimilation system, *Q. J. R. Meteorol. Soc.*, *137*(656), 553–597, doi:10.1002/qj.828.

Druyan, L. M. (2011), Studies of 21st-century precipitation trends over West Africa, *Int. J. Climatol.*, *31*(10), 1415–1424, doi:10.1002/joc.2180.

Gbobaniyi, E., et al. (2013), Climatology, annual cycle and interannual variability of precipitation and temperature in CORDEX simulations over West Africa, *Int. J. Climatol.*, *34*, 2241–2257, doi:10.1002/joc.3834.

Giorgi, F., C. Jones, and G. R. Asrar (2009), Addressing climate information needs at the regional level: The CORDEX framework, *WMO Bull.*, *58*(3), 175–183.

Haarsma, R. J., F. M. Selten, S. L. Weber, and M. Kliphuis (2005), Sahel rainfall variability and response to greenhouse warming, *Geophys. Res. Lett.*, *32*, L17702, doi:10.1029/2005GL023232.

Hastenrath, S. (2000), Interannual and longer term variability of upper-air circulation over the tropical Atlantic and West Africa in boreal summer, *Int. J. Climatol.*, *20*(12), 1415–1430, doi:10.1002/1097-0088(200010)20:12<1415::AID-JOC550>3.0.CO;2-C.

Hawkins, E., and R. Sutton (2009), The potential to narrow uncertainty in regional climate predictions, *Bull. Am. Meteorol. Soc.*, *90*(8), 1095–1107, doi:10.1175/2009BAMS2607.1.

Held, I. M., T. L. Delworth, J. Lu, K. L. Findell, and T. R. Knutson (2005), Simulation of Sahel drought in the 20th and 21st centuries, *Proc. Natl. Acad. Sci. U.S.A.*, *102*(50), 17,891–17,896, doi:10.1073/pnas.0509057102.

Hewitson, B., C. Lennard, G. Nikulin, and C. Jones (2012), CORDEX-Africa: A unique opportunity for science and capacity building, *CLIVAR Exch.*, *60*, 6–7.

Hoerling, M., J. Hurrell, J. Eischeid, and A. Phillips (2006), Detection and attribution of twentieth-century Northern and Southern African rainfall change, *J. Clim.*, *19*(16), 3989–4008, doi:10.1175/JCLI3842.1.

James, R., and R. Washington (2013), Changes in African temperature and precipitation associated with degrees of global warming, *Clim. Change*, *117*, 859–872, doi:10.1007/s10584-012-0581-7.

James, R., R. Washington, and D. P. Rowell (2013), Implications of global warming for the climate of African rainforests, *Philos. Trans. R. Soc. London, Ser. B*, *368*(1625), 20120298, doi:10.1098/rstb.2012.0298.

James, R., R. Washington, and D. P. Rowell (2014), African climate change uncertainty in perturbed physics ensembles: Implications of global warming to 4 °C and beyond, *J. Clim.*, *27*(12), 4677–4692, doi:10.1175/JCLI-D-13-00612.1.

Jenkins, G. S., A. T. Gaye, and B. Sylla (2005), Late 20th century attribution of drying trends in the Sahel from the Regional Climate Model (RegCM3), *Geophys. Res. Lett.*, *32*, L22705, doi:10.1029/2005GL024225.

Jones, C., F. Giorgi, and G. Asrar (2011), The Coordinated Regional Downscaling Experiment: CORDEX, an international downscaling link to CMIP5, *CLIVAR Exch. 56*, *16*(2), 34–40.

Jones, R. G., M. Noguer, D. C. Hassel, D. Hudson, S. S. Wilson, G. J. Jenkins, and J. F. B. Mitchell (2004), *Generating High Resolution Climate Change Scenarios Using PRECIS*, Met Office Hadley Centre, Exeter, U. K.

Jones, R. G., A. Hartley, C. McSweeney, C. Mathison, and C. Buontempo (2012), Deriving high resolution climate data for West Africa for the period 1950–2100, *UNEP-WCMC Tech. Rep.*

Kalnay, E., M. Kanamitsu, R. Kistler, W. Collins, D. Deaven, L. Gandin, M. Iredell, S. Saha, G. White, and J. Woollen (1996), The NCEP/NCAR 40-year reanalysis project, *Bull. Am. Meteorol. Soc.*, *77*(3), 437–471, doi:10.1175/1520-0477(1996)077<0437:TNYRP>2.0.CO;2.

Lau, K. M., S. S. P. Shen, K.-M. Kim, and H. Wang (2006), A multimodel study of the twentieth-century simulations of Sahel drought from the 1970s to 1990s, *J. Geophys. Res.*, *111*, D07111, doi:10.1029/2005JD006281.

Marsham, J. H., N. S. Dixon, L. Garcia-Carreras, G. M. S. Lister, D. J. Parker, P. Knippertz, and C. E. Birch (2013), The role of moist convection in the West African monsoon system: Insights from continental-scale convection-permitting simulations, *Geophys. Res. Lett.*, *40*, 1843–1849, doi:10.1002/grl.50347.

Massey, N., R. Jones, F. E. L. Otto, T. Aina, S. Wilson, J. M. Murphy, D. Hassell, Y. H. Yamazaki, and M. R. Allen (2014), Weather@home—development and validation of a very large ensemble modelling system for probabilistic event attribution, *Q. J. R. Meteorol. Soc.*, doi:10.1002/qj.2455.

McSweeney, C. F., R. G. Jones, and B. B. B. Booth (2012), Selecting ensemble members to provide regional climate change information, *J. Clim.*, *25*(20), 7100–7121, doi:10.1175/JCLI-D-11-00526.1.

McSweeney, C. F., R. G. Jones, R. W. Lee, and D. P. Rowell (2014), Selecting CMIP5 GCMs for downscaling over multiple regions, *Clim. Dyn.*, doi:10.1007/s00382-014-2418-8.

Meynadier, R., O. Bock, S. Gervois, F. Guichard, J.-L. Redelsperger, A. Agustí-Panareda, and A. Beljaars (2010), West African Monsoon water cycle: 2. Assessment of numerical weather prediction water budgets, *J. Geophys. Res.*, *115*, D19107, doi:10.1029/2010JD013919.

Monerie, P., B. Fontaine, and P. Roucou (2012a), Expected future changes in the African monsoon between 2030 and 2070 using some CMIP3 and CMIP5 models under a medium-low RCP scenario, *J. Geophys. Res.*, *117*, D16111, doi:10.1029/2012JD017510.

Monerie, P., P. Roucou, and B. Fontaine (2012b), Mid-century effects of climate change on African monsoon dynamics using the A1B emission scenario, *Int. J. Climatol.*, doi:10.1002/joc.3476.

Murphy, J. M., B. B. B. Booth, M. Collins, G. R. Harris, D. M. H. Sexton, and M. J. Webb (2007), A methodology for probabilistic predictions of regional climate change from perturbed physics ensembles, *Philos. Trans. R. Soc. London, Ser. A*, *365*(1857), 1993–2028, doi:10.1098/rsta.2007.2077.

Nicholson, S. E. (2009), A revised picture of the structure of the monsoon and land ITCZ over West Africa, *Clim. Dyn.*, *32*(7–8), 1155–1171, doi:10.1007/s00382-008-0514-3.

Nicholson, S. E., and J. P. Grist (2003), The seasonal evolution of the atmospheric circulation over West Africa and Equatorial Africa, *J. Clim.*, *16*(7), 1013–1030, doi:10.1175/1520-0442(2003)016<1013:TSEOTA>2.0.CO;2.

Nikulin, G., et al. (2012), Precipitation climatology in an ensemble of CORDEX-Africa regional climate simulations, *J. Clim.*, *25*(18), 6057–6078, doi:10.1175/JCLI-D-11-00375.1.

Pope, V. D., M. L. Gallani, P. R. Rowntree, and R. Stratton (2000), The impact of new physical parametrizations in the Hadley Centre climate model: HadAM3, *Clim. Dyn.*, *16*(2–3), 123–146, doi:10.1007/s003820050009.

Sylla, M. B., A. T. Gaye, G. S. Jenkins, J. S. Pal, and F. Giorgi (2010), Consistency of projected drought over the Sahel with changes in the monsoon circulation and extremes in a regional climate model projections, *J. Geophys. Res.*, *115*, D16108, doi:10.1029/2009JD012983.

Tarhule, A. A. (2007), Climate information for development: An integrated dissemination model, *Afr. Dev.*, *XXXII*(4), 127–138, doi:10.4314/ad.v32i4.57325.

Taylor, K. E., R. J. Stouffer, and G. A. Meehl (2012), An overview of CMIP5 and the experiment design, *Bull. Am. Meteorol. Soc.*, *93*(4), 485–498, doi:10.1175/BAMS-D-11-00094.1.

Tokinaga, H., and S. Xie (2011), Weakening of the equatorial Atlantic cold tongue over the past six decades, *Nat. Geosci.*, *4*(4), 222–226, doi:10.1038/ngeo1078.

Vizy, E. K., and K. H. Cook (2002), Development and application of a mesoscale climate model for the tropics: Influence of sea surface temperature anomalies on the West African monsoon, *J. Geophys. Res.*, *107*(D3), 4023, doi:10.1029/2001JD000686.

Vizy, E. K., K. H. Cook, J. Crétat, and N. Neupane (2013), Projections of a wetter Sahel in the twenty-first century from global and regional models, *J. Clim.*, *26*(13), 4664–4687, doi:10.1175/JCLI-D-12-00533.1.

Washington, R., R. James, H. Pearce, W. M. Pokam, and W. Moufouma-Okia (2013), Congo Basin rainfall climatology: Can we believe the climate models?, *Philos. Trans. R. Soc. London, Ser. B*, *368*(1625), doi:10.1098/rstb.2012.0296.

